Food Chemistry 204 (2016) 37–45

Contents lists available at ScienceDirect

Food Chemistry

journal homepage: www.elsevier.com/locate/foodchem

Chemical profile of mango (*Mangifera indica* L.) using electrospray ionisation mass spectrometry (ESI-MS)

Bruno G. Oliveira [a], Helber B. Costa [a], José A. Ventura [b], Tamara P. Kondratyuk [c], Maria E.S. Barroso [d], Radigya M. Correia [a], Elisângela F. Pimentel [d], Fernanda E. Pinto [a], Denise C. Endringer [d,e], Wanderson Romão [a,e,*]

[a] Laboratório de Petroleômica e Química Forense, Departamento de Química, Universidade Federal do Espírito Santo (UFES), Avenida Fernando Ferrari, 514, Goiabeiras, Vitória, ES CEP: 29075-910, Brazil
[b] Instituto Capixaba de Pesquisa, Assistência Técnica e Extensão Rural (INCAPER), R. Afonso Sarlo, 160 – Bento Ferreira, Vitoria, ES 29052-010, Brazil
[c] University of Hawaii at Hilo, The Daniel K. Inouye College of Pharmacy, HI, USA
[d] Universidade Vila Velha-UVV, Rua Comissário José Dantas de Melo, 21, Boa Vista 29102-770, Espírito Santo, Brazil
[e] Instituto Federal do Espírito Santo (IFES), Av. Ministro Salgado Filho, Soteco, Vila Velha, ES 29106-010, Brazil

ARTICLE INFO

Article history:
Received 15 October 2015
Received in revised form 16 February 2016
Accepted 16 February 2016
Available online 17 February 2016

Keywords:
Mangifera indica L.
Mango
Chemical profile
Mass spectrometry
ESI(−)FT-ICR MS

ABSTRACT

Mangifera indica L., mango fruit, is consumed as a dietary supplement with purported health benefits; it is widely used in the food industry. Herein, the chemical profile of the Ubá mango at four distinct maturation stages was evaluated during the process of growth and maturity using negative-ion mode electrospray ionisation Fourier transform ion cyclotron resonance mass spectrometry (ESI(−)FT-ICR MS) and physicochemical characterisation analysis (total titratable acidity (TA), total soluble solids (TSS), TSS/TA ratio, and total polyphenolic content). Primary (organic acids and sugars) and secondary metabolites (polyphenolic compounds) were mostly identified in the third maturation stage, thus indicating the best stage for harvesting and consuming the fruit. In addition, the potential cancer chemoprevention of the secondary metabolites (phenolic extracts obtained from mango samples) was evaluated using the induction of quinone reductase activity, concluding that fruit polyphenols have the potential for cancer chemoprevention.

1. Introduction

The mango (*Mangifera indica* L. Anacardiaceae) is one of the most commercialised fruits in tropical countries. Over 1000 different varietals of mangoes are produced worldwide. Mangoes have several biological activities and are also considered a nutraceutical fruit (Masibo & He, 2009).

In 2008, approximately 1.2 million mangoes were produced in Brazil, and more than 40,000 tonnes were exported (Food, 2009). The Ubá mango is one type of cultivar that is produced in Brazil. This cultivar is mainly produced in the State of Minas Gerais (MG), in the region of Zona da Mata (Ribeiro, Barbosa, Queiroz, Knödler, & Schieber, 2008) and in the State of Espirito Santo (ES). In the last region, the Institute Capixaba of Research, Technical Assistance, and Rural Extension (INCAPER) developed a plantation in 2010 (INCAPER, 2013)) with 1600 hectares of planted area, generating five thousand tons of mangoes annually. The production of Ubá mangoes for the purpose of processing is promising for the State of Espírito Santo, due to the current demand of the world market for pulp and fruit juice (INCAPER, 2010).

The Ubá mango is a small fruit that can weigh up to 150 g, and approximately 13% of its mass is comprised of the peel, which is yellowish and firm when it is ripe. The pulp has short, thin, and soft fibres (Ramos et al., 2005). Furthermore, the fruit has a pale-yellow colour after processing, appropriate viscosity for consumption, and good conservation of the flavour. Because of these sensorial qualities, the Ubá mango has been widely used by industry for the production of pulp and juices, as well as consumption *in natura* by the population (Ribeiro et al., 2008).

The harvesting of the mango is a decisive step that can compromise the entire production. The mango is a climacteric fruit; however, if it is harvested at a very green maturity stage, i.e., before physiologic maturity, the fruit will have a high level of acidity. Nevertheless, if it is harvested at a late maturity stage, it will suffer greater damage in the process of harvesting and transportation

* Corresponding author at: Laboratório de Petroleômica e Química Forense, Departamento de Química, Universidade Federal do Espírito Santo (UFES), Avenida Fernando Ferrari, 514, Goiabeiras, Vitória, ES CEP: 29075-910, Brazil.
E-mail address: wandersonromao@gmail.com (W. Romão).

http://dx.doi.org/10.1016/j.foodchem.2016.02.117
0308-8146/

(Rivera et al., 2014). No studies have been reported in the literature linking the chemical profile of the Ubá mango, its physicochemical properties, and the best period or stage for harvesting. Harvesting takes into consideration several of the fruit's characteristics, e.g., the peel colour, the pulp, and the physical shape, as well as some chemical parameters, such as the pH, total titratable acidity (TA), total soluble solids (TSS), fruit density, and latex aspects (Rivera et al., 2014).

Mass spectrometry (MS) techniques, such as Fourier transform ion cyclotron resonance mass spectrometry (FT-ICR MS), allow the identification of chemical constituents in complex organic mixtures (Dias, Dixini, et al., 2015; Dias, Pereira, et al., 2015; Nascimento et al., 2015). FT-ICR MS combined with an electrospray ionisation (ESI) source has been applied in metabolomics studies, and it has proved to be an excellent approach to control the quality of fruits (Costa et al., 2015). High-resolution MS enables the separation and detection of thousands of ions produced by specific compounds (Ghislain, Faure, & Michels, 2012). This technique provides accurate important information, such as the elemental formula ($C_cH_hN_nO_o$), double bond equivalent (DBE), isotopologue profile, and chemical connectivity (from collision induced dissociation (CID) experiments). Herein, the physicochemical characterisation of the Ubá mango was evaluated at four different stages of maturation during the process of growth and maturity. Subsequently, primary and secondary metabolites were identified using ESI(−)FT-ICR MS. The potential cancer chemoprevention of the secondary metabolites (phenolic extracts obtained from mango samples) was evaluated using the induction of quinone reductase activity.

2. Experiment

2.1. Sample and reagents

M. indica L. mango samples at four different stages of maturation were collected by Capixaba Institute for Research, Technical Assistance, and Rural Extension (INCAPER) in the city of Colatina in Espirito Santo, Brazil. The harvesting was done by an experienced technical team during the year 2015. To distinguish between the four stages of maturation, the fruit's characteristics were categorised in triplicate for each maturation stage into physicochemical criteria, e.g., peel colour, firmness, physical shape and latex appearance. All samples were washed with chlorinated water and rinsed with distilled water. Physicochemical characteristics were measured for all fruits and then the fruits were stored at −20 °C.

2.2. Physicochemical analysis

Analyses of the pH, TA (g citric acid equivalent/100 g of pulp), TSS (°Bx), and TSS/TA ratio were performed. The pH and TSS were measured using a pH metre (Metron® model 827) and a refractometer (Abbé 2 WAJ with readings that ranged from 1.300 to 1.72 nD with 0–95 °Bx). The TA measurements were performed using a 0.1 mol L^{-1} NaOH solution (Sigma-Aldrich; St Louis, MO) as the titrant. Finally, the TSS/TA ratio was calculated, to evaluate the quality of the pulp. All analyses were done in triplicate and performed in accordance with methods described by Instituto Adolfo Lutz (2005).

2.3. Preparation of the glycoside fraction

For the analysis of sugar and organic acids, the fruit pulp was homogenised in a blender in the proportion of 1 g of pulp to 1.5 mL of methanol/water (50% *v*/*v*). The fraction was then subsequently filtered by a filter paper (Unifil® black stripe 125 mm) to extract both the fibrous portion and any material not solubilised.

2.4. Preparation of the phenolic fraction

For the extraction of the phenolic compounds, we used an adapted methodology from Talcott and Talcott (2009). A portion of 20 g of pulp was crushed using a domestic blender. Then, the extract was placed in an amber flask with 60 mL of a solution containing methanol/ethanol/acetone (1:1:1 *v*/*v*/*v*) and submitted to an ultrasonic bath (frequency of 40 kHz) for one hour. Subsequently, the extract was filtered using a qualitative paper (Unifil® black stripe 125 nm). To increase the efficiency of the extraction method, the process was repeated twice over the pulp remaining on the paper using 45 and 30 mL of solution, consecutively, reaching a final volume of ≈135 mL.

The filtered extracts were concentrated and the solvent evaporated using a rotary evaporator. Methanol (30 mL) was added to the extract and centrifuged at 2500 RCF fora period of 10 min to precipitate the pectin. The procedure was repeated again over the precipitate and 20 mL of methanol were added. The solvent was removed from the rotary evaporator and the mango extract was washed with 15 mL of water in a cartridge (Waters Corporation, Milford, MA) composed of 360 mg of C18, to remove sugars, and to concentrate the phenolic compounds. Before the washing of extract, the cartridge was conditioned with injections of 30 and 50 mL of methanol and water, respectively. Subsequently, the phenolic compounds were extracted from the cartridge using 20 mL of methanol solution (25 v/v%) and subsequently evaporated and brought to a total volume of 8 mL.

2.5. ESI(−)FT-ICR MS

For glycoside fraction analysis, 10 μL of the extract containing primary metabolics were dissolved with 1 mL of methanol/water solution (50% *v*/*v*). Subsequently, the solution was doped with 5 μL of internal standard, deuterated glucose (D-Glucose-1, 2, 3, 4, 5, 6, 6-d7) solution at 5 mmol L^{-1}, and finally basified with 4 μL of NH_4OH (Vetec Fine Chemicals Ltda, Brazil).

For the extract rich in phenolic compounds, 500 μL of the extract were dissolved with 500 μL of methanol and doped with 10 μL of deuterated glucose solution. Then, the final solution was basified with 4 μL of NH_4OH and directly infused at a flow rate of 6 μL min^{-1} into the ESI(−) source.

The mass spectrometer (model 9.4 T Solarix; Bruker Daltonics, Bremen, Germany) was set to negative ion mode, ESI(−), over a mass range of *m*/*z* 150–1500. The ESI source conditions were as follows: a nebuliser gas pressure of 1.4 bar, a capillary voltage of 3.8 kV, and a capillary transfer temperature of 200 °C. Ion time accumulation was 0.010 s. ESI(−)FT-ICR mass spectra were acquired by accumulating 32 scans of time-domain transient signals in 16 mega-point time-domain data sets. All mass spectra were externally calibrated using NaTFA (*m*/*z* from 200 to 1200). Resolving power, $m/\Delta m_{50\%}$ = 1,000,000 (in which $\Delta m_{50\%}$ is the full peak width at the half-maximum peak height of *m*/*z* 400) and a mass accuracy of <1–2 ppm provided the unambiguous molecular formula assignments for singly charged molecular ions.

Mass spectra were acquired and processed using Data Analysis software (Bruker Daltonics, Bremen, Germany). Elemental compositions of the compounds were determined by measuring the *m*/*z* values. The proposed structures for each formula were assigned using the ChemSpider (www.chemspider.com) database. The degree of unsaturation for each molecule can be deduced directly from its *DBE* value according to equation $DBE = c - h/2 + n/2 + 1$, where *c*, *h*, and *n* are the numbers of carbon, hydrogen, and nitrogen atoms, respectively, in the molecular formula.

The tandem mass spectrometry (MS^2) experiments were performed on a quadrupole analyser coupled to the FT-ICR mass spectrometer. The ESI(−)-MS/MS spectra were acquired using an infusion flow rate of 5 μL min^{-1}, capillary voltage of 3.0 kV, nebulising temperature of 250 °C, argon as collision gas, ion accumulation time of 1 s, isolation window of 1.0 (*m*/*z* units), and 25–45% of the collision energy.

2.6. Total polyphenolic content

The analysis of the phenolic fraction was performed using a UV/Vis spectrophotometer (Model 482; Femto, São Paulo, Brazil). Total polyphenol contents (TPC) were determined using Folin-Ciocalteu reagent (Sigma-Aldrich). Absorbance was registered at 715 nm. TPC assay was performed according to Brazilian Pharmacopeia (FARM. BRAS, 2002). A five-point analytical curve was built using concentrations of gallic acid anhydrous standard solutions (from 1.1 to 17.4 μg mL^{-1}). The curves showed satisfactory linearity within the analysed range (r^2 = 0.996). Phenolic fractions sample analyses were performed in triplicate.

2.7. Determination of quinone reductase activity in cell cultures

The activity of quinone reductase of phenolic fractions was assessed in 96-well plates using Hepa 1c1c7 (murine hepatoma cells, ATCC CRL-2026), as previously described. Briefly, cells were grown to a density of 2×10^4 cells mL^{-1} in 200 μL of MEM-a containing 5% antibiotic–antimycotic (Gibco, Thermo-Fisher) and 10% foetal bovine serum at 37 °C in a 5% CO_2 atmosphere. After a 24-h pre-incubation period, the media were changed and cells were treated with the indicated sample or control concentrations. The cells were incubated with test samples for an additional 48 h. QR activity was measured as a function of the NADPH-dependent menadiol-mediated reduction of 3-(4,5-dimethylthiazo-2-yl)-2,5-diphenylte trazolium bromide (MTT) to a blue formazan. Protein content was determined *via* the crystal violet staining of identical plates. Specific activity is defined as nmol of formazan formed per mg protein per min. The induction ratio (*IR*) of QR activity represents the specific enzyme activity of agent-treated cells compared with a DMSO-treated control. The concentration to double activity (*CD*) was determined through a dose response assay for active substances (*IR* > 2). Data presented are the results of three independent experiments run in duplicate. 4-Bromoflavone (*CD* = 0.01 nM) was used as a positive control. The chemoprevention index ($CI = IC_{50}/CD$) was also determined. Data were processed using non-linear regression analysis (TableCurve 2D V4; Systat Software, San Jose, CA)

2.8. Statistical analysis

Analysis of variance and Tukey's post hoc test were used to statistically evaluate the differences among mean values of the relative intensity of signals obtained for the four stages of maturation. Differences were considered significant if $p < 0.05$. The statistical analyses were conducted using Assistat 7.7 Beta.

3. Results and discussion

3.1. Physicochemical analysis

Four stages of maturation of the Ubá mango were analysed. The mangoes were grouped in accordance with the TSS, TA, peel colour, pulp colour, and firmness. The physical characteristics of mangoes for each stage were: (i) stage 1: dark green colour peel, rigid light yellow flesh, and low moisture content; (ii) stage 2: light green colour peel, rigid light yellow flesh, and average moisture content; (iii) stage 3: yellowish green colour peel, soft yellow pulp, and high moisture content; and (iv) stage 4: yellow peel, very soft and disintegrating yellow internal flesh, characteristic of the late stage of maturity (Kienzle et al., 2012) (Fig. 1S, supplementary material).

The physicochemical properties (pH, TA, TSS (°Bx), and TSS/TA ratio) results are displayed in Fig. 1 and Table 1S (supplementary material). Mangoes at stage 1 presented the lowest TSS value (7.1 °Bx), Fig. 1a. This value increases until stage 3, when a value of around 16.5 ° Bx is reached. This value is similar to those reported in other studies (Ribeiro et al., 2008; Rivera et al., 2014). The increase in TSS could be explained by amylase's action on starch, resulting in the production of soluble sugars, such sucrose, glucose and fructose (Nambi, Thangavel, & Jesudas, 2015). At stage 4, there was a small reduction in TSS values (14.5 °Bx) Fig. 1a), due to the advanced stage of maturation (Rivera et al., 2014).

High TA values (1.83 g/100 g) were observed in mangoes in stage 1 as well as the lowest pH values (pH = 3.01). The TA values decrease over the development and maturation process, reaching 0.33 g/100 g of pulp at stage 4 (Fig. 1b). As a consequence, the pH values increased (Fig. 1c) (Rivera et al., 2014). The acidity is attributed to the organic acids often found in free form or associated with salts, esters, and glycosides. A reduction of these acids is common as the fruit develops and ripens (Nambi, Thangavel, & Jesudas, 2015; Rivera et al., 2014). Therefore, an increase in TSS and a reduction in TA lead to an increase in the SST/TA ratio (Fig. 1d).

3.2. ESI(−)FT-ICR MS

3.2.1. Glycoside fraction analysis

ESI(−)FT-ICR mass spectra were obtained to evaluate the chemical profile of the Ubá mango samples over the four maturation stages (Fig. 2). The acquisition conditions of the ESI source were maintained constant in all analyses. The dopant added in all analyses was detected as a deuterated glucose dimer, $[C_{12}H_{10}D_{14}O_{12} - H]^-$ ion of *m*/*z* 373 (compound 7). Sucrose or its isomers were detected in its deprotonated form and as chlorine adduct, $[C_{12}H_{22}O_{11} + H]^-$ and $[C_{12}H_{22}O_{11} + Cl]^-$ ions of *m*/*z* 341 (compound 4) and 377 (compound 8), respectively. Additionally, sucrose/glucose dimers and trimers were also detected as $[C_{18}H_{33}O_{17}]^-$, $[C_{24}H_{43}O_{22}]^-$ and $[C_{36}H_{65}O_{33}]^-$ ions of *m*/*z* 521 (compound 20), 683 (compound 25) and 1025 (compound 27), respectively.

Sucrose and fructose are the main carbohydrates detected in mangoes. Studies have assessed changes in levels of these compounds in mangoes from other cultivars, such as Van Dyke, Tommy, Palmer and Hadem (Bernardes-Silva, Lajolo, & Cordenunsi, 2003). In general, a higher signal/noise ratio and an abundance of these signals are shown for mango samples at maturation stages 3 and 4 (Fig. 2c–d). where the relative intensity of the internal standard is reduced. Table 2S shows the chemical structure, molecular formulas, theoretical *m*/*z* values, mass errors, and *DBE*s of chemical species detected in Fig. 2.

The presence of sucrose/glucose dimers and trimers during the ionisation process using the ESI(−) source can be explained based on cluster formation during electrospray ionisation (Nascimento et al. 2015). To confirm this hypothesis, the ESI(−)FT-ICR mass spectrum was acquired for a solution of sucrose standard at 20% *m*/*v*, doped with 5 μL of deuterated glucose (Fig. 2S). The ions of *m*/*z* 521, 683, and 1025 that correspond to clusters of glucose were again produced, similar to the behaviour observed in Fig. 2.

In addition to sugars, two acid species were detected in the deprotonated form: shikimic (*m*/*z* 173) and citric (*m*/*z* 191) acids, detected with mass errors of 0.31 and 0.37 ppm, respectively, and *DBE* = 3, Fig. 2 and Table 2S. Citric acid is the predominant acid in mangoes (Hossain, Rana, Kimura, & Roslan, 2014), and shikimic acid is a precursor in the synthesis of phenolic compounds (Moreno, Benavides, Zevallos, & Velázquez, 2012).

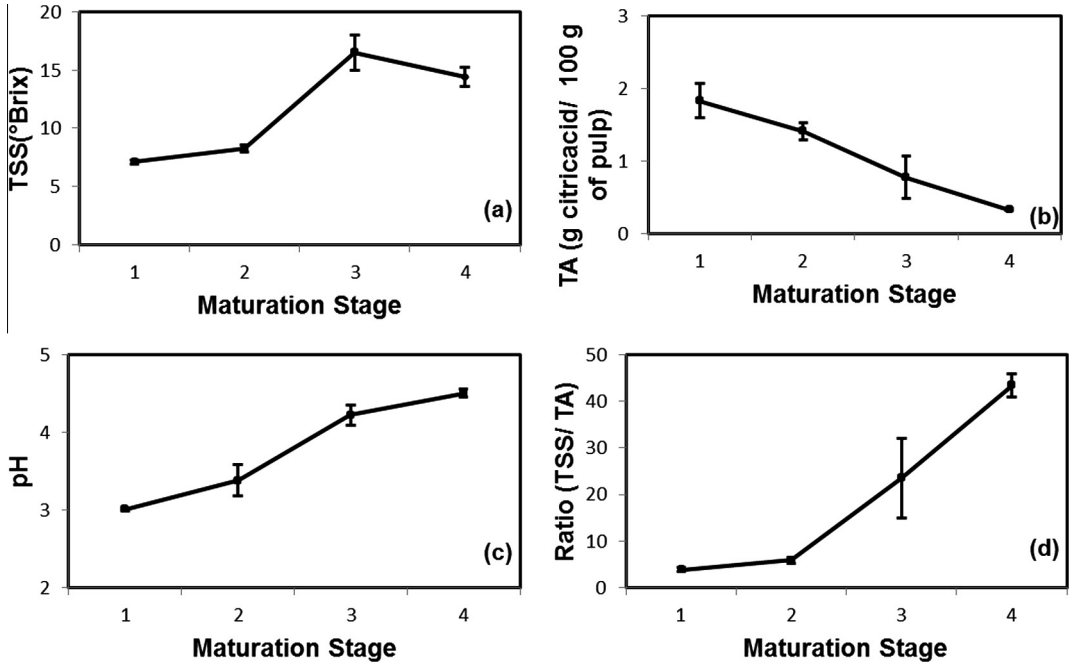

Fig. 1. Physicochemical properties ((a) TSS, (b) TA, (c) pH, and (d) TSS/TA ratio) of the Ubá mango at various maturation stages.

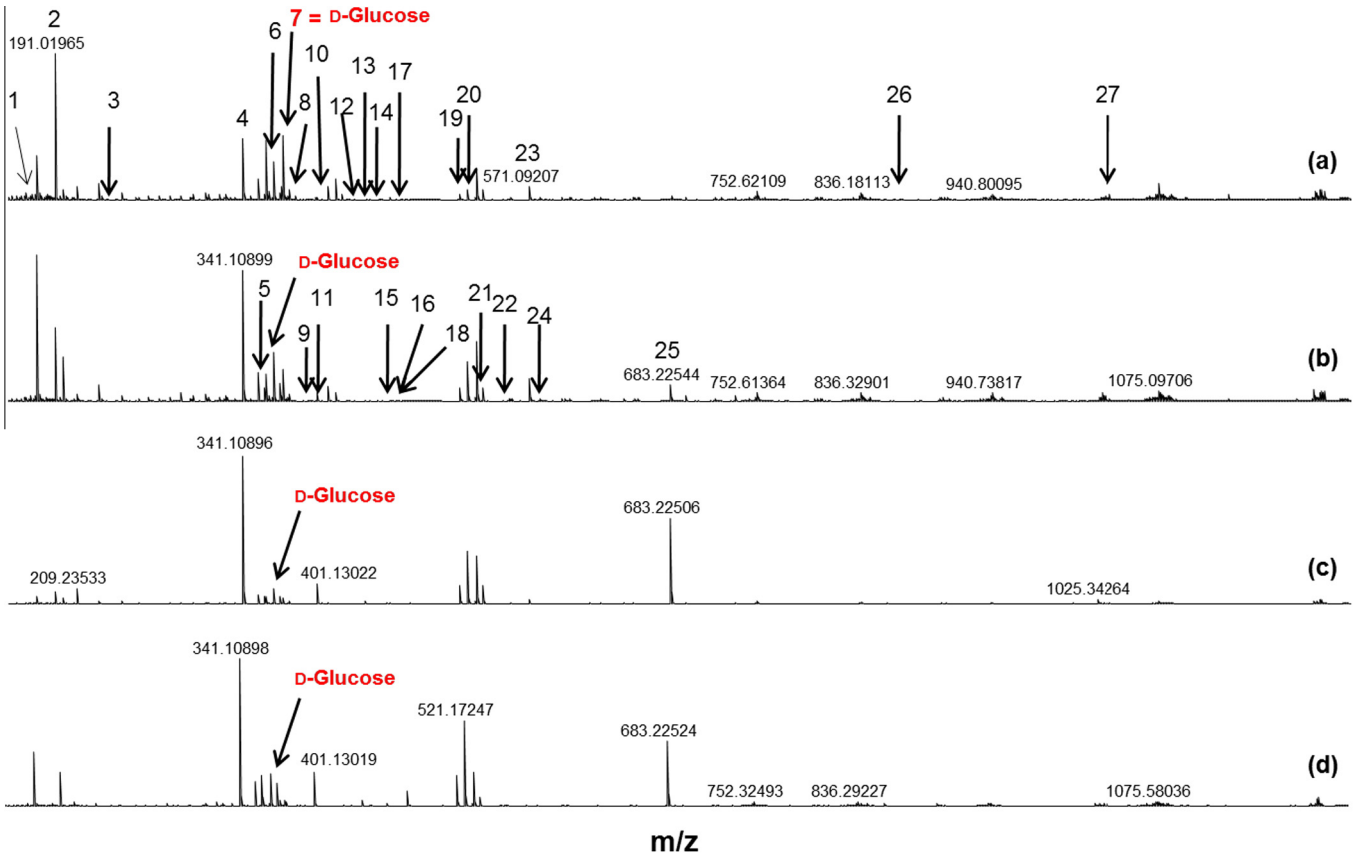

Fig. 2. ESI(−)FT-ICR MS for the glycoside fraction of Ubá mango samples at various maturation stages ((a) 1, (b) 2, (c) 3 and (d) 4). Note that a higher abundance of sucrose, its dimers and trimers are observed for mango samples at maturation stages 3 and 4. As consequence, a higher ionic suppression is observed for the internal standard of *m*/*z* 373.

To confirm the structures and the connectivity of the ions of *m*/*z* 341, 377, 521, 683, and 1025, ESI(+)-MS/MS spectra were acquired (Fig. 3Sa–e). Initially, the CID experiments for the ion of *m*/*z* 341 generates the fragment of *m*/*z* 179 ($[C_5H_{12}O_6]^-$ ion), Fig. 3Sa. This is due to a neutral loss of hexose. ESI(−)MS/MS for the ion of *m*/*z* 377 shows HCl (36 Da) elimination producing the fragment of *m*/*z* 341 (Fig. 3Sb). Ions of *m*/*z* 521 and 683 (Fig. 3Sc and d) both produce the fragment of *m*/*z* 341 due to glucose (180 Da) and sucrose

(342 Da) losses, respectively. Finally, the ESI(−)MS/MS for the ion of *m*/*z* 1025 produces fragments of *m*/*z* 683 and 341 (Fig. 3Se).

It is important to monitor the sugar and organic acid contents to ensure the sensory attributes in mangoes, specifically the flavour, is a balance between the contents of sugars and organic acids (Sivakumar, Jiang, Yahia, & Elhadi, 2011). Variations in the relative abundance of sucrose and its cluster isomers as well as organic (shikimic (*m*/*z* 173) and citric (*m*/*z* 191)) acids are graphically shown in Fig. 3. Sucrose and its clusters were expressed as the ratio of the sum of their absolute intensities (*m*/*z* 341, 377, 521, 683, and 1025) divided by the absolute intensity of the deuterated glucose signal (*m*/*z* 373). Similarly, the relative intensity of organic acids was expressed as the ratio of the sum of their absolute intensities (*m*/*z* 173 and 191) to that of the internal standard (*m*/*z* 373).

Similar to the results displayed in Fig. 1 and Table 1S, an increase in the sucrose content or its isomers was observed during the development and ripening of the fruit until stage 3, and subsequently, a reduction in stage 4 (Fig. 3). The increased sucrose concentration can be explained by the conversion of starch into sugars that occurs during fruit ripening (Nambi et al., 2015), and the reduction of the sucrose content in stage 4 can be attributed to the aging of the fruit, where sugar degradation occurs (Nambi et al., 2015; Rivera et al., 2014). Stages 3 and 4 have higher sugar levels than stages 1 and 2; this difference was considered statistically significant, as reported by Tukey's test (Fig. 3). Therefore, stages 3 and 4 are responsible for mango sweetness. On the other hand, despite the fact that shikimic and citric acids are more abundant in stages 1 and 2, their absolute values do not differ statistically during the maturity stages (Fig. 3). This could be explained by either the small amount of detected acids or the small number of replicates. In general, ESI(−)FT-ICR MS data predict, at a molecular level, the results of physicochemical conventional assays, thus diagnosing the chemical species responsible for the variations in the TSS, TA, pH, and TSS/TA ratio of the Ubá mango.

3.2.2. Analysis of the phenolic fraction

ESI(−)FT-ICR mass spectra were acquired to evaluate the content of phenolic compounds of Ubá mango samples at the four maturation stages (Fig. 4a–d). Eight phenolic compounds were identified in their deprotonated form, $[M-H]^-$ ions: methyl gallate or gallic acid derivatives, $[C_8H_7O_5]^-$ ions of *m*/*z* 183 (compound 1), ellagic acid or its isomers, $[C_{14}H_5O_8]^-$ ions of *m*/*z* 300 (compound 2), glucogallin or gallic acid derivatives, $[C_{13}H_{15}O_{10}]^-$ ions of *m*/*z* 331 (compound 3), methyl digallate ester, $[C_{15}H_{11}O_9]^-$ ions of *m*/*z* 335 (compound 4), mangiferin, $[C_{19}H_{17}O_{11}]^-$ ions of *m*/*z* 421 (compound 5), digalloyl glucose, $[C_{20}H_{19}O_{14}]^-$ ions of *m*/*z* 483 (compound 6), trigalloyl glucose, $[C_{27}H_{23}O_{18}]^-$ ions of *m*/*z* 635 (compound 7),and tetragalloyl glucose, $[C_{34}H_{27}O_{22}]^-$ ions of *m*/*z* 787 (compound 8). In all cases, a high mass accuracy was obtained with less than 2 ppm error (Table 3S). It was also observed that with an increase in the molar mass of phenolic compounds, the *DBE* values increase, ranging from 5 to 21, corresponding to species containing 1–4 phenolic rings (Table 3S).

The chemical structure of phenolic compounds (Table 3S) are confirmed from ESI(−)MS/MS experiments (Fig. 4S). In general, for most ions, neutral losses of the galloyl fraction (152 Da) and of gallic acid (170 Da) were observed, Fig. 4Sa, c–e. The fragmentation profile found for these polyphenolic compounds is associated with gallotannins and benzophenone derivatives (Berardini, Carle, & Schieber, 2004).

In this study, seven tannins and one xanthone were identified. Ellagic acid is a common tannin in mangoes and has been identified in other cultivars of mangoes (Arogba, 2000; Pierson et al., 2014). Ellagic acid has anti-inflammatory (Corbett et al., 2010), gastroprotective (Beserra et al., 2011), cardioprotective (Warpe, Mali, Arulmozhi, Bodhankar, & Mahadik, 2015), and antioxidant activities (Priyadarsini, Khopde, Kumar, & Mohan, 2002).

Other tannins identified, e.g., methyl gallate, galloyl glucose, methyl digallate ester, digalloyl glucose, trigalloyl glucose, and tetragalloyl glucose, are also presented in other cultivars of mangoes (Pierson et al., 2014). These tannins were described as having antimicrobial (Arbos, Stevani, & Castanha, 2013), antibacterial (Engels, Gänzle, & Schieber, 2012) and antifungal activities (Bruneton, 2005). Mangiferin is a glycosylated xanthine found in several varieties of mango. It is reported to have pharmacological activity in various organs and tissues, protecting the heart, neurons, liver, and kidneys and preventing or delaying the onset of diseases (Morais et al., 2012).

The abundance of phenolic compounds detected by ESI(−)-FT-ICR MS (Fig. 4) was compared to shikimic acid as function of maturation stage (Fig. 5). The shikimic acid (*m*/*z* 173) detected in the glycoside fraction of fruit (Fig. 2) is a phenolic compound precursor (Ghosh, Chisti, & Banerjee, 2012). Fig. 5 shows a decrease in the content of shikimic acid as a consequence of an increase in the intensity of phenolic species over the course of maturation (1 → 4), confirming the conversion of shikimic acid into phenolic compounds (Fig. 5).

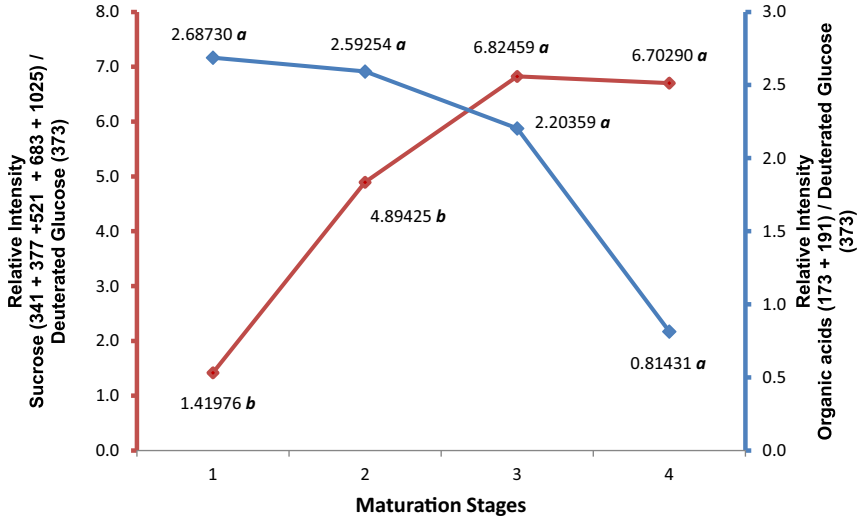

Fig. 3. Relative intensity of sucrose and organic acids of Ubá mango at various maturation stages. Different letters mean that for Tukey's test with $p < 0.05$, the relative intensity values are significantly different.

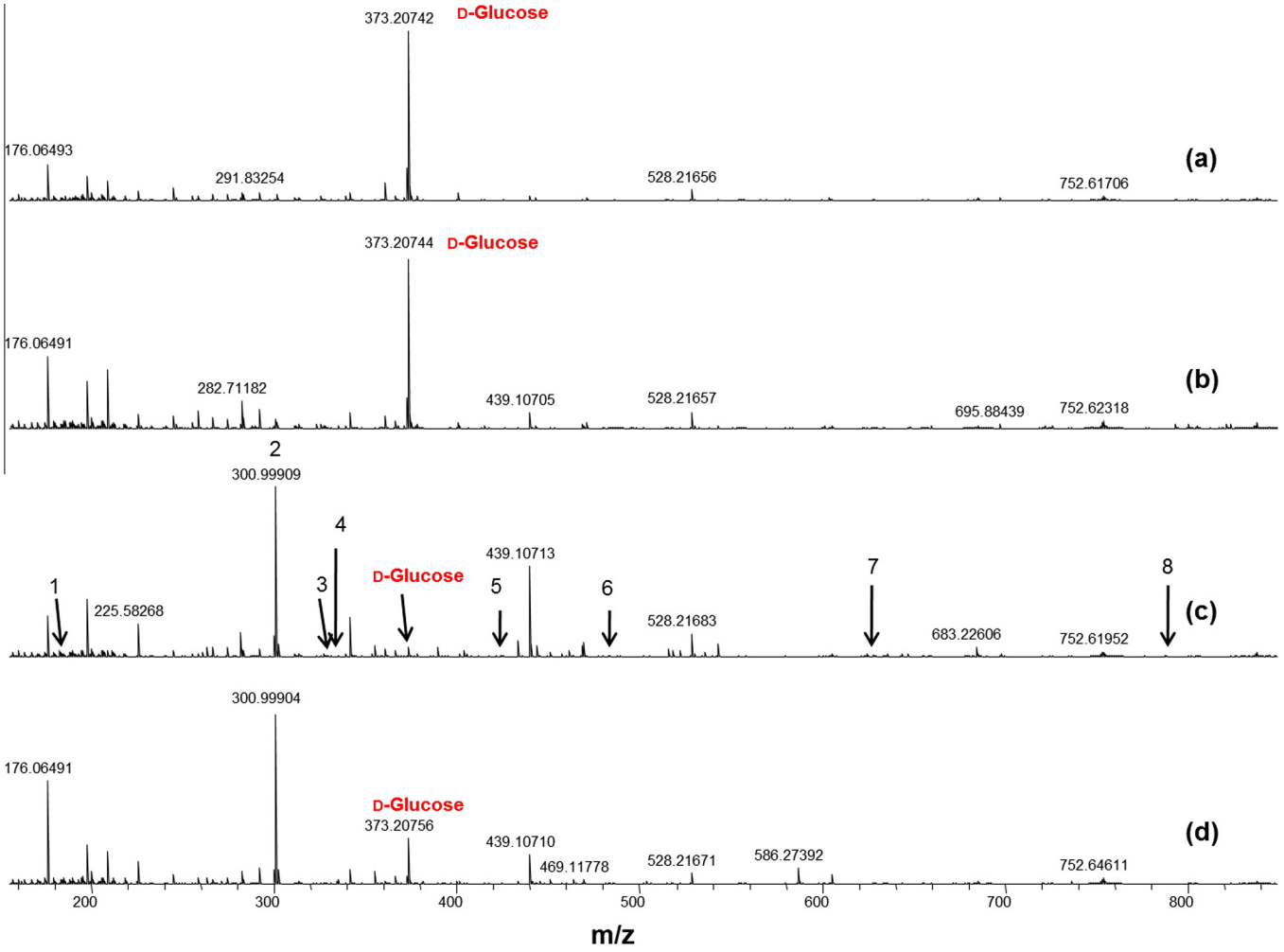

Fig. 4. ESI(−)FT-ICR MS for the phenolic fraction of Ubá mango samples at various maturation stages ((a) 1, (b) 2, (c) 3 and (d) 4). Note that a higher abundance of phenolic species (*m*/*z* 183, 300, 331, 335, 421, 483, 635 e 787) are revealed for mango samples at maturation stages 3 and 4. As consequence, a higher ionic suppression is observed for the internal standard of *m*/*z* 373.

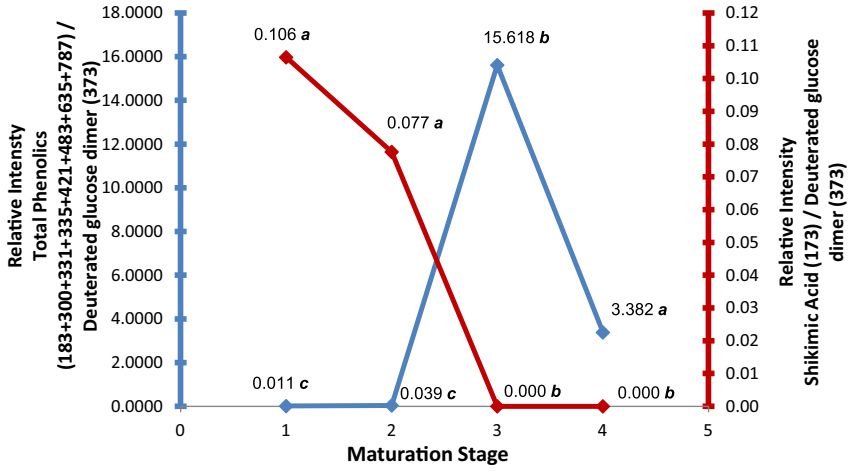

Fig. 5. Relative intensity of shikimic acid and of all phenolic compounds detected at various maturation stages of the Ubá mango. Different letters mean that the values are significantly different with $p < 0.05$.

The statistical analysis from Tukey's test indicates that the phenolic contents of stages 3 and 4 differ significantly from each other as well as from stages 1 and 2 (Fig. 5). It is possible to conclude that stages 1 and 2 are poor in phenolic compounds. It was observed that as the mangoes developed and ripened, the amount of these molecules increased in stage 3

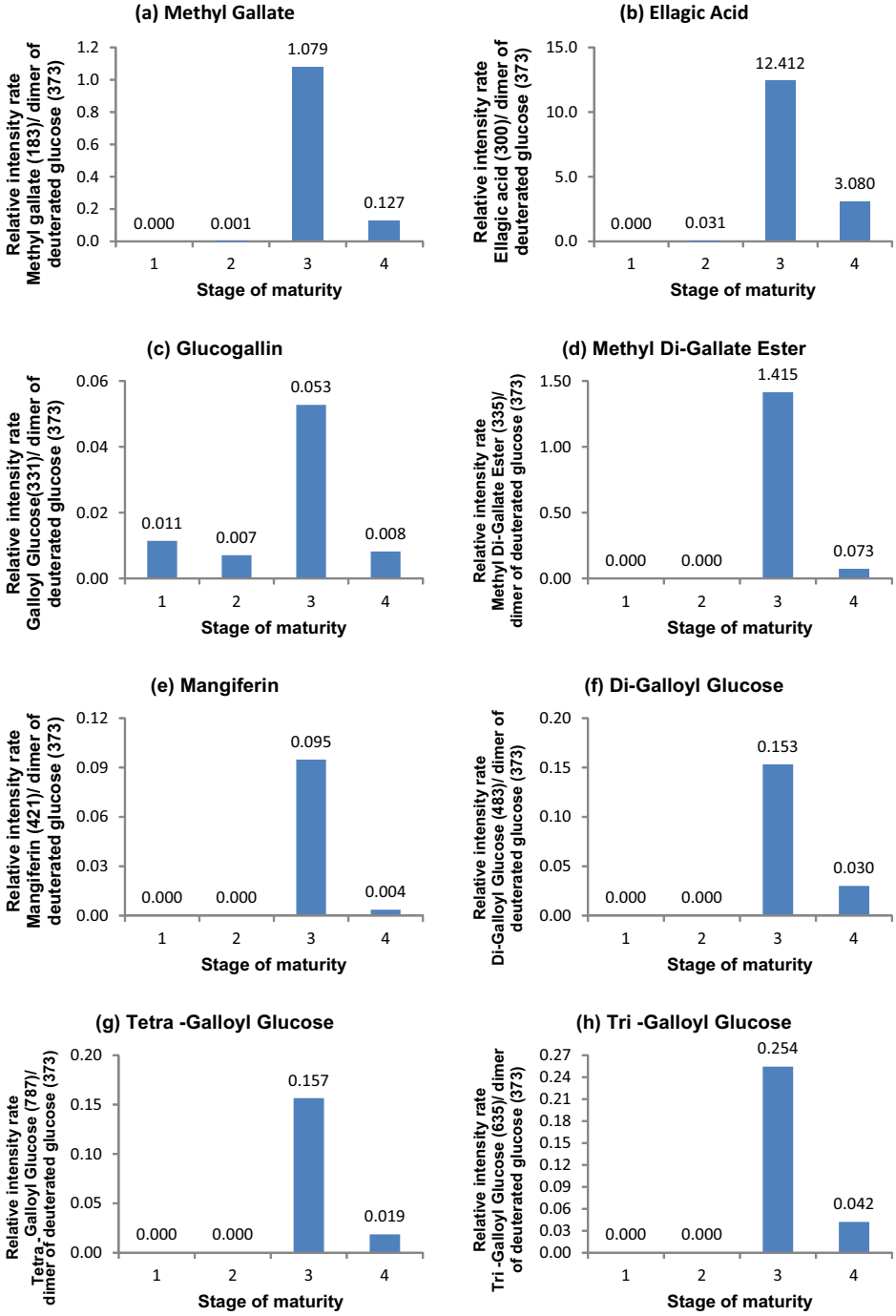

Fig. 6. Relative intensity of phenolic compounds at various maturation stages.

and showed a subtle decrease in stage 4. These results were similar to those of Palafox and colleagues (2012) for phenolic compounds in Ataulfo mangoes. The total phenols quantification corroborated the ESI(−)FT-ICR MS data (Table 4S), where stages 3 and 4 have higher values of phenolic compounds than stages 1 and 2.

The abundance of each phenolic compound by ESI(−)-FT-ICR MS was also evaluated according to the maturation stage. The relative intensity of each compound was determined by the ratio of its absolute intensity to the intensity of deuterated glucose (m/z 373, Fig. 6). In general, methyl gallate, ellagic acid, mangiferin, digalloyl glucose, trigalloyl glucose, and tetragalloyl glucose have abundance values that differ across the maturation stages. Methyl gallate (Fig. 6a) had a more prominent relative intensity signal (≈1.1) in stage 3, and this differed statistically from stages 1 and 2, indicating higher concentrations of this compound at stage 3. Similarly, ellagic acid (Fig. 6b) had a greater relative intensity signal at stage 3 (≈12.4) and stage 4 (≈3.08), statistically differing from stages 1 and 2, indicating higher concentrations of the compound in stages 3 and 4. Mangiferin, digalloyl glucose, tetragalloyl glucose and trigalloyl glucose (Fig. 6e–h, respectively) had high relative intensity signals at stage 3 (≈0.95, 0.15, 0.26, and 0.16, respectively), and these values differed statistically from stages 1, 2, and 4, indicating higher concentrations of the compound at stage 3. Glucogallin and methyl ester digallate are unique in that their relative intensity values did not differ statistically at different

stages of maturation, (Fig. 6c and d), although they had higher values of abundance at stage 3 (≈0.1 and 1.4, respectively).

3.2.3. Induction of quinone reductase activity

The total polyphenol concentration differed among the maturation stages, Table 4S. The induction of quinone reductase in cell cultures is known to be a fast and sensitive *in vitro* test for the analysis of the induction of the detoxification potential Phase 2 enzyme (Kinghorn et al., 2004). Quinone reductase is responsible for the detoxification of the quinone cycle, causing a reduction of hydroquinones, the applicant process in the initial phase of carcinogenesis (Kinghorn et al., 2004). Stage 1 had induction ratio higher than 2.0, with a *CD* of 2.37 ± 0.01 ng polyphenols/g of fresh fruit. The IC_{50} was higher than 62.4 ng of polyphenols/g of fresh fruit, yielding a *CI* higher than 26. Several compounds present in the Ubá mango showed activity in the induction of quinone reductase, including flavonoids (Kinghorn et al., 2004). It was also noted that flavonoid glycosides induce quinone reductase *in vivo*, due to conversion to the aglycone, a derivative with biological activity (Carcache-Blanco et al., 2004).

4. Conclusions

The ultra-high resolution and mass accuracy spectrometry with Fourier transform (FT-ICR MS) enabled validation of the results obtained through physicochemical conventional tests, such as TSS, TA, pH, and SST/TA ratio at the four maturation stages of the Ubá mango. ESI(−)FT-ICR MS showed the variations in the contents of organic acids, sugars, and phenolic compounds. Evaluating these results, it was concluded that mangoes at stage 3 are rich in sugars and have a higher content of phenolic compounds. In addition, the polyphenols of the fruits of *M. indica* have the potential for cancer chemoprevention; however, further assays need to be conducted.

Acknowledgements

The authors thank FAPES (65921208/2014), CAPES (23038.007083/2014-40), and CNPq (445987/2014-6, 401409/2014-7 and 314453/2014/8) for their financial support.

Appendix A. Supplementary data

Supplementary data associated with this article can be found, in the online version, at http://dx.doi.org/10.1016/j.foodchem.2016.02.117.

References

Arbos, K. A., Stevani, P. C., & Castanha, R. F. (2013). Atividade antimicrobiana, antioxidante e teor de compostos fenólicos em casca e amêndoa de frutos de manga. *Revista Ceres, 60*(2), 161–165.

Arogba, S. S. (2000). Mango (*Mangiferaindica*) kernel: chromatographic analysis of the tannin, and stability study of the associated polyphenol oxidase activity. *Journal of Food Composition and Analysis, 13*(2), 149–156.

Berardini, N., Carle, R., & Schieber, A. (2004). Characterization of gallotannins and benzophenone derivatives from mango (Mangifera indica L. cv. 'Tommy Atkins') peels, pulp and kernels by high-performance liquid chromatography/electrospray ionization mass spectrometry. *Rapid Communications in Mass Spectrometry, 18*, 2208–2216.

Bernardes-Silva, A. P. F., Lajolo, F. M., & Cordenunsi, B. R. (2003). Evolução dos teores de amido e açúcares solúveis durante o desenvolvimento e amadurecimento de diferentes cultivares de manga. *Ciência e Tecnologia de Alimentos, 23*, 116–120.

Beserra, A. M., Calegari, P. I, Souza Mdo, C., Dos Santos, R. A., Lima, J. C., Silva, R. M., ... Martins, D. T. (2011). Gastroprotective and ulcer-healing mechanisms of ellagic acid in experimental rats. *Journal of Agricultural and Food Chemistry, 59*(13), 6957–6965.

Bruneton, J. (2005). Elementos de Fitoquímica y de Farmacognosia, Acribia (Ed.), SA: Espanha, 1991.

Carcache-Blanco, E. J., Kang, Y. H., Park, E. J., Su, B. N., Kardono, L. B., Riswans, S., ... Kinghorn, A. D. (2004). Constituents of the stem bark of Pongamia pinnata with the potential to induce quinone reductase. *Journal of Natural Products, 66*(9), 1197–1202 [Erratum. In: Journal of Natural Products, 2004, 67(1), 126].

Corbett, S., Daniel, J., Drayton, R., Field, M., Steinhardt, R., & Garrett, N. (2010). Evaluation of the anti-inflammatory effects of ellagic acid. *Journal of Peri Anesthesia Nursing, 25*(40), 214–220.

Costa, H. B., Souza, L. M., Soprani, L. C., Oliveira, B. G., Ogawa, E. M., Korres, A. M. N., ... Romão, W. (2015). Monitoring the physicochemical degradation of coconut water using ESI-FT-ICR MS. *Food Chemistry, 174*, 139–146.

Dias, H. P., Dixini, P. V., Almeida, L. C. P., Vanini, G., Castro, E. V. R., Aquije, G. M. F. V., ... Romão, W. (2015). Evidencing the crude oil corrosion by Raman spectroscopy, atomic force microscopy and electrospray ionization FT-ICR mass spectrometry. *Fuel, 139*, 328–336.

Dias, H. P., Pereira, T. M. C., Vanini, G., Dixini, P. V. M., Celante, V. G., Castro, E. V. R., ... Romão, W. (2015). Monitoring the degradation and the corrosion of naphthenic acids by electrospray ionization Fourier transform ion cyclotron resonance mass spectrometry and atomic force microscopy. *Fuel, 126*, 85–95.

Engels, C., Gänzle, M. G., & Schieber, A. (2012). Fast LC–MS analysis of gallotannins from mango (*Mangiferaindica* L.) kernels and effects of methanolysis on their antibacterial activity and iron binding capacity. *Food Research International, 45*(1), 422–426.

Food and Agriculture Organization (FAO) (2009). Produção e Exportação: citação da base de dados. URL <http://apps.fao.org/>. Accessed 20-02-2015. Farmacopéia Brasileira IV (2002). São Paulo, Atheneu.

Ghislain, T., Faure, P., & Michels, R. (2012). Detection and monitoring of PAH and Oxy-PAHsby high resolution mass spectrometry: Comparison of ESI, APCI and APPI source detection. *Journal of the American Society of Mass Spectrometry, 23*, 530–536.

Ghosh, S., Chisti, Y., & Banerjee, U. C. (2012). Production of shikimic acid. *Biotechnology Advances, 30*, 1425–1431.

Hossain, A., Rana, M., Kimura, Y., & Roslan, H. A. (2014). Changes in biochemical characteristics and activities of ripening associated enzymes in mango fruit during the storage at different temperatures. *BioMed Research International, 14*, 1–11.

INCAPER (Instituto capixaba de Pesquisa, assistência Técnica e Extenção Rural). Manga diversifica atividades agrícolas no Espírito Santo, 2013. URL <http://www.incaper.es.gov.br/noticia_completa.php?id=3229>. Accessed 10-01-2015.

INCAPER (Instituto capixaba de Pesquisa, assistência Técnica e Extenção Rural). Desenvolvimento da Fruticultura. Informativo Especial do INCAPER. URL <http://incaper.web407.uni5.net/revista.php?idcap=978>. Accessed 20-08-2014.

Instituto Adolfo Lutz. Normas analíticas do Instituto Adolfo Lutz. IV – Métodos químicos e físicos para análise de alimentos (2005). São Paulo. Secretária de Estado da Saúde, Coordenadoria dos Serviços Especializados.

Kienzle, S., Sruamsiri, P., Carle, R., Sirisakulwat, S., Spreer, W., & Neidharta, S. (2012). Harvest maturity detection for 'Nam Dokmai #4' mango fruit (*Mangiferaindica* L.) in consideration of long supply chains. *Postharvest Biology and Technology, 72*, 64–75.

Kinghorn, A. D., Su, B. N., Jang, D. S., Chang, L. C., Lee, D., Gu, J. Q., ... Pezzuto, J. M. (2004). Natural inhibitors of carcinogenesis. *Planta Medica, 70*, 691–705.

Palafox, H. C., Yahia, E., Osuna, M. A. I., Martinez, P. G., Sánchez, M. R., & Aguilar, G. A. G. (2012). Effect of ripeness stage of mango fruit (*Mangiferaindica* L., cv. Ataulfo) on physiological parameters and antioxidant activity. *Scientia Horticulturae, 135*, 7–13.

Masibo, M., & HE, Q. (2009). Mango bioactive compounds and related nutraceutical properties – A review. *Food Review International, 25*, 346–370.

Morais, T. C., Lopes, S. C., Carvalho, K. M. M. B., Arruda, B. R., Souza, F. T. C., Trevisan, M. T. S., ... Santos, F. A. (2012). Mangiferin, a natural xanthone, accelerates gastrointestinal transit in mice involving cholinergic mechanism. *World Journal of Gastroenterology, 18*(25), 3207–3214.

Moreno, A. B., Benavides, J., Zevallos, L. C., & Velázquez, D. A. J. (2012). *Journal of Agricultural and Food Chemistry, 60*, 11378–11386.

Nambi, V. E. K., Thangavel, D., & Jesudas, M. (2015). Scientific classification of ripening period and development of colour grade chart for Indian mangoes (Mangiferaindica L.) using multivariate cluster analysis. *Scientia Horticulturae, 193*, 90–98.

Nascimento, I. R., Costa, H. B., Souza, L. M., Soprani, L. C., Merlo, B. B., & Romão, W. (2015). Chemical identification of cannabinoids in street marijuana samples using electrospray ionization FT-ICR mass spectrometry. *Analytical Methods, 7*, 1415–1424.

Pierson, J. T., Monteith, G. R., Roberts-Thomson, S. J., Dietzgen, R. G., Gidley, M. J., & Shaw, P. N. (2014). Phytochemical extraction, characterisation and comparative distribution across four mango (*Mangiferaindica* L.) fruit varieties. *Food Chemistry, 149*, 253–263.

Priyadarsini, K. I., Khopde, S. M., Kumar, S. S., & Mohan, H. (2002). Free radical studies of ellagic acid, a natural phenolic antioxidant. *Journal of Agricultural and Food Chemistry, 50*(7), 2200–2206.

Ramos, A. M., Couto, F. A. A., Rezende, P. M., Lelis, F. M. V, Benevides, S. D., &Perez, R. (2005).Manga Ubá. Boas Práticas Agrícolas para a Produção Destinada à Agroindústria. Editora UFV.

Ribeiro, S. M. R., Barbosa, L. C. A., Queiroz, J. H., Knödler, M., & Schieber, A. (2008). Phenolic compounds and antioxidant capacity of Brazilian mango (Mangiferaindica L.) varieties. *Food Chemistry, 110*(3), 620–626.

Rivera, N. V., Blasco, J., Pérez, J. C., Domínguez, G. C., Perea-Flores, M. J. P., Vázquez, I. A., ... Rebollo, R. F. (2014). Computer vision system applied to classification of "manila" mangoes during ripening process. *Food and Bioprocess Technology, 7*, 1183–1794.

Sivakumar, D., Jiang, Y., Yahia & Elhadi, M. (2011). Maintaining mango (Mangiferaindica L.) fruit quality during the export chain. *Food Research International, 44*(5), 1254–1263.

Talcott, S., & Talcott, S. (2009). Phytochemical attributes contribute to the health-promoting benefits of mangoes. Final Research Report to the National Mango Board. Texas A&M University, Department of Nutrition and Food Science.

Warpe, V. S., Mali, V. R., Arulmozhi, S., Bodhankar, S. L., & Mahadik, K. R. (2015). Cardioprotective effect of ellagic acid on doxorubicin induced cardiotoxicity in wistar rats. *Journal of Acute Medicine, 5*(1), 1–8.